Solar Energy Materials 6 (1982) 151–158
North-Holland Publishing Company

TEMPERATURE DEPENDENCE OF SILICON SOLAR CELL CHARACTERISTICS†

N. D. ARORA* and J. R. HAUSER
Department of Electrical Engineering,
North Carolina State University,
Raleigh, NC 27650, USA

Received 12 August 1981

The effects of temperature on the characteristics of p–n junction solar cells are investigated theoretically. An exact numerical model of the semiconductor transport equations is used to calculate the output parameters of the cell taking into account temperature effect on the material parameters of the cell. These calculations show that the temperature coefficient of solar cell parameters such as open-circuit voltage, short-circuit current, efficiency, etc., are typically nonlinear over the range of temperature (300–450 K) studied in agreement with the experimental results as against a constant value obtained by simple calculations.

1. Introduction

Recently, different basic approaches have been used to reduce the cost of terrestrial photovoltaic systems. One of these is the use of concentrating sunlight to increase the solar cell output power. The inherent increase in the operating temperature of the solar cell induced by high levels of illumination degrades cell performance. The effect of increasing operating temperature on the characteristics of a silicon solar cell has been studied both experimentally and theoretically by various investigators [1–7]. However, the results of these investigations are not always consistent because of various parameters of actual solar cells being functions of temperature and moreover simplified calculations are normally used to explain the observed temperature effect. In order to realistically calculate the temperature coefficient of the characteristics like open-circuit voltage V_{oc}, short-circuit current I_{sc}, maximum efficiency η_{max}, etc., of an actual solar cell it is necessary to use numerical methods for solving the transport equations [7, 8] and take into account temperature effects on the material parameters.

In this paper we report the results of calculation of the temperature dependence of the characteristic of a conventional silicon solar cell using numerical analysis taking into account Auger recombination, band-gap narrowing, graded impurity profiles and position dependent mobility in the diffused layers [9]. Other physical phenomena

*On leave of absence from Solid State Physics Laboratory, Lucknow Road, Delhi-110007, India.

†This work was supported in part by a research grant from the Solar Energy Research Institute, Golden, CO.

0165-1633/82/0000–0000/$02.75

like series resistance of the cell, reflection losses at the front surface of the cell, surface recombination losses at the front and back surface are also included in these calculations. Finally, the temperature variations of the absorption coefficient of light, lifetime and mobility are taken into account.

These calculations show that the normalized temperature coefficient of the output parameters of an actual solar cell are not constant as is found by simple calculations but varies with temperature in agreement with experimental results.

2. Theory

Conventional silicon solar cells consist of a uniformly doped p type substrate of thickness l having a heavily doped n^+ diffused layer of thickness d with a complimentary error function profile. A metal grid contact structure is made on the front (diffused side) while the backside is fully covered by a metal contact. The front surface has an antireflection coating to reduce the reflection losses at the front.

To calculate the characteristic of such a cell, the cell is modelled as a one-dimensional structure. The transport and continuity equation in the diffused region for low levels of injection may be written as

$$\frac{dp}{dx} = -\frac{J_p(x)}{qV_t\mu_p(x)} - \frac{p}{N_{eff}}\frac{dN_{eff}}{dx}, \tag{1}$$

$$\frac{1}{q}\frac{dJ_p}{dx} = -\frac{1}{\tau_p(x)}\left(p - \frac{n_i^2}{N_{eff}}\right) + G(x), \tag{2}$$

where $J_p(x)$ is the hole current density, p is the hole concentration at x, $\mu_p(x)$ is the hole mobility (function of impurity concentration), N_{eff} is the effective doping level (obtained from the actual doping using the bandgap reduction formulation [9]), n_i is the intrinsic carrier concentration, q is the electron change ($=1.6\times10^{-19}c$) and $V_t = kT/q$. The hole lifetime τ_p at a distance x is calculated both from Auger band-to-band recombination and recombination via trapping centers and is given by [9]

$$\frac{1}{\tau_p(x)} = C_n N^2 + \left(1 + \frac{N}{N_0}\right)\Big/\tau_0. \tag{3}$$

Here C_n is the Auger recombination coefficient ($=0.8\times10^{-31}$ cm^{6}s^{-1}). The constant $N_0(=4.27\times10^{17}$ cm$^{-3})$ is independent of the diffused layer while τ_0 depends on it [9]. The optical generation rate $G(x)$ at a distance x in the cell is given by

$$G(x) = \int_{\lambda_1}^{\lambda_2} F_0(\lambda)\alpha(\lambda)(1 - R(\lambda))\, e^{-\alpha x}\, d\lambda, \tag{4}$$

where $F_0(\lambda)\, d\lambda$ is the number of photons in the light incident on the cell in the wavelength interval $d\lambda$, $\alpha(\lambda)$ is the absorption coefficient while $R(\lambda)$ is the reflection coefficient from the cell's front surface at wavelength λ and λ_1, λ_2 are the limits of spectral sensitivity of the cell.

These equations are then solved numerically to calculate the current density J_p using a technique described elsewhere [9]. The base being uniformly doped, the current density J_n in the base is calculated analytically using the following expression [10]

$$J_n = \int_{\lambda_1}^{\lambda_2} \frac{qF_0(1-R)\alpha L_n e^{-\alpha(d+W)}}{\alpha^2 L_n^2 - 1} \{\alpha L_n - z\}\, d\lambda, \tag{5}$$

where

$$z = \frac{S_n\left(\cosh\frac{l}{L_n} - e^{-\alpha l}\right) + \frac{D_n}{L_n}\left(\sinh\frac{l}{L_n} + \alpha L_n e^{-\alpha l}\right)}{S_n \sinh\frac{l}{L_n} + \frac{D_n}{L_n}\cosh\frac{l}{L_n}}$$

and L_n is the diffusion length in the base, D_n is the diffusion coefficient, S_n is the surface recombination velocity at the back while w is the depletion width. The photocurrent collection takes place from the depletion region as well, and the current density J_{dep} due to this is given by [9]

$$J_{dep} = \int_{\lambda_1}^{\lambda_2} qF_0(1-R)\, e^{-\alpha d}(1 - e^{-\alpha W}) d\lambda. \tag{6}$$

Thus, the total photocurrent is

$$I_L = (J_n + J_p + J_{dep})A_e,$$

where A_e is the effective area of the cell exposed to light.

When the cell is connected to the load the current passing through the load is

$$I = I_L - I_d, \tag{7}$$

where I_d is the dark current of the diode given by

$$I_d = I_{01}[e^u - 1] + I_{02}[e^{u/2} - 1], \tag{8}$$

with $u = (v + I_d R_s / v_t)$, and R_s is the series resistance of the cell. The first term on the right side of eq. (8) is the recombination current in the neutral region while the second term is that due to recombination in the depletion region. The series resistance R_s is calculated using the following approximate expression [11]

$$R_s = \frac{\rho_B l}{A_a} + \frac{R_\square}{12n}\left(\frac{a}{LF}\right) + \frac{\rho_m LF}{2SF \times TH}, \tag{9}$$

where ρ_B is the resistivity of the base layer, $R_\square$ is the sheet resistance of the surface layer, ρ_m is the resistivity of the grid material, n is the number of fingers, a is the spacing between the fingers. LF is the finger length, TH is the thickness, SF is the width, and A_a is the actual area of the cell.

The material parameters which are functions of temperature and which effect the operation of the solar cell are intrinsic carrier density n_i, mobility μ, diffusion length

L_n, diffusion coefficient D_n and absorption coefficient α. All these parameters are taken as functions of temperature and incorporated into eqs. (1)–(9).

3. Results and discussion

The results to be presented here are based on p–n junction solar cells, the structure of which corresponds to a typical currently available high efficiency cell. The cell has been assumed to have a thickness of 300 μm and 0.3 μm junction depth with a 600 Å thickness of Ta_2O_5 for an antireflection layer. The base and surface doping densities are assumed to have values of 1.3×10^{15} and 2×10^{20} cm^{-3}, respectively. The front contact has 24 grid fingers with a bus bar having 94% active area for a cell of 2×2 cm^2. The diffusion length L_n in the base is assumed to be 200 μm at 300 K and this changes to 236 μm at 450 K [12]. The variation of mobility with temperature and concentration is taken into account according to the theory given by Li and Thurber [13, 14]. The variation of α with temperature is taken from experimental data of Weakliem and Redfield [15] with room temperature data taken from Phillip and Taft [16]. The value of $F_0(\lambda)$ for both AM0 and AM1 is obtained from the spectral irradiance data given in ref. [17]. The reflection coefficient $R(\lambda)$ is computed from the known thickness of the antireflection coating and its index of refraction [18].

3.1. Short-circuit current I_{sc}

The variation of I_{sc} with temperature, calculated using eqs. (7) and (8), for AM0 and AM1 solar spectrums is shown in fig. 1. It is seen that there is a slight increase in I_{sc} with temperature for both AM0 and AM1 although the rate of increase is lower at AM1 as compared to AM0. Further, the increase in I_{sc} with temperature is not linear as simple calculations show, but is a nonlinear function of temperature. The higher the temperature, the lower the temperature coefficient. This nonlinear behavior of I_{sc} has been reported by Goldhammer et al. [5]. The calculated temperature coefficients of various solar cell parameters along with reported experimental results are compiled in table 1. As can be seen the agreement between the calculated and observed temperature coefficient of I_{sc} is very good. This small positive temperature coefficient of I_{sc} is mainly due to an increase in the minority carrier lifetime and an increase in the optical generation rate with temperature with the later effect being the most important influence on the increase of I_{sc}. This also explains the lower temperature coefficient at the higher temperatures because at higher temperatures the increase of optical generation rate slows down.

3.2. Open circuit voltage V_{oc}

The open circuit voltage V_{oc}, again calculated using eqs. (7) and (8), for the AM0 and AM1 spectrums is shown in fig. 1 as a function of temperature. The decrease of V_{oc} with increasing temperature is mainly due to an increase in n_i with temperature. This is the reason why the rate of decrease of V_{oc} is the same for both AM0 and AM1.

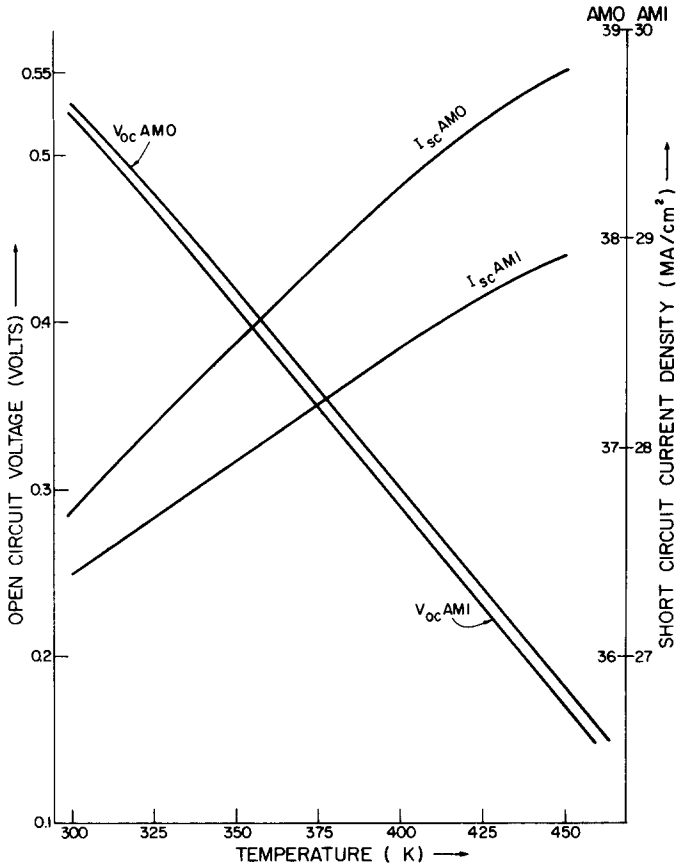

Fig. 1. Variation of open circuit voltage (V_{oc}) and short-circuit current (I_{sc}) of n^+p silicon solar cell with temperature at AM0 and AM1 solar spectrum.

Table 1
Temperature coefficients of V_{oc}, I_{sc} and η_{max} for 10 Ω cm conventional silicon solar cell and AM0 solar spectrum

	Temperature (°C)		$\frac{1}{I_{sc}}\frac{dI_{sc}}{dT}$	$\frac{dV_{oc}}{dT}$	$\frac{1}{\eta_{max}}\frac{d\eta_{max}}{dT}$
	T_0	ΔT	(%/°C)	(mV/°C)	(%/°C)
Luft [1]	28	10–80	0.072	−2.28	
Curtain and Cool [4]	25	15–55	0.053	−2.26	
Goldhammer and Slifer [5]	25	25–100	(0.046–0.042)	−(2.28–2.31)	
Our calculations	25	25–100	(0.045–0.0427)	−(2.24–2.31)	−(0.543–0.555)

The higher rate of decrease at higher temperature arises because the space charge recombination current becomes comparable to that due to neutral region recombination. The calculated negative temperature coefficient of V_{oc} for AM0 solar spectrum is given in table 1 along with experimentally observed value. As can be seen the agreement is good.

3.3. Maximum conversion efficiency η_{max}

The conversion efficiency η_{max} of the cell is obtained using

$$\eta_{max} = \mathrm{FF}\, I_{sc} V_{oc} / A_a P_i, \tag{10}$$

where FF is the fill factor, A_a is the actual area of the cell ($=4$ cm^2) and P_i is the incidence solar irradiance which is 135.3 mW/cm^2 for AM0 and 88.9 mW/cm^2 for AM1 [17] solar spectrums.

The efficiency calculated using eq. (9) for AM0 and AM1 solar spectrums are plotted in fig. 2. As can be seen, the decrease in η_{max} with temperature is a nonlinear function of temperature, with the temperature coefficient of η_{max} larger at higher temperatures. Further, the rate of decrease is larger for AM1 than for AM0. From fig. 1 it is seen that the values of V_{oc} and I_{sc} are higher for AM0 as compared to AM1, because of a larger power input for AM0, but the efficiency for AM0 is lower than that for AM1. This is because of the removal of most of the ultraviolet portions of the spectrum by the atmosphere, channeling the sun's energy more and more toward the visible region where the spectral response is higher. Simple calculations show [19] that $\eta_{max} T$ is constant, but this is far from reality as can be seen from our calculations. In practice $\eta_{max} T$ goes on decreasing with increasing temperature. The temperature coefficient of η_{max} at 50°C for AM0 is 0.543%/°C.

Study of figs. 1 and 2 indicates that parameters of the cell deteriorates rapidly with increasing temperatures. It is thus clear that the performance of Si p–n junction solar cell at 400 K is only 44% of the cell performance at 300 K.

4. Conclusion

The effects of temperature on the characteristic of an actual solar cell have been studied. It is found that the temperature variations of the parameters of the cell are in general nonlinear functions of temperature. The temperature coefficient of I_{sc} decreases while that of V_{oc} and η_{max} increases with increasing temperature. The theoretical results are in very good agreement with experimental results when account is taken of the temperature variations of all the solar cell parameters.

Acknowledgement

One of the authors (NDA) is grateful to Dr. S. C. Jain, Director, Solid State Physics Laboratory for his keen interest and encouragement during the course of the work.

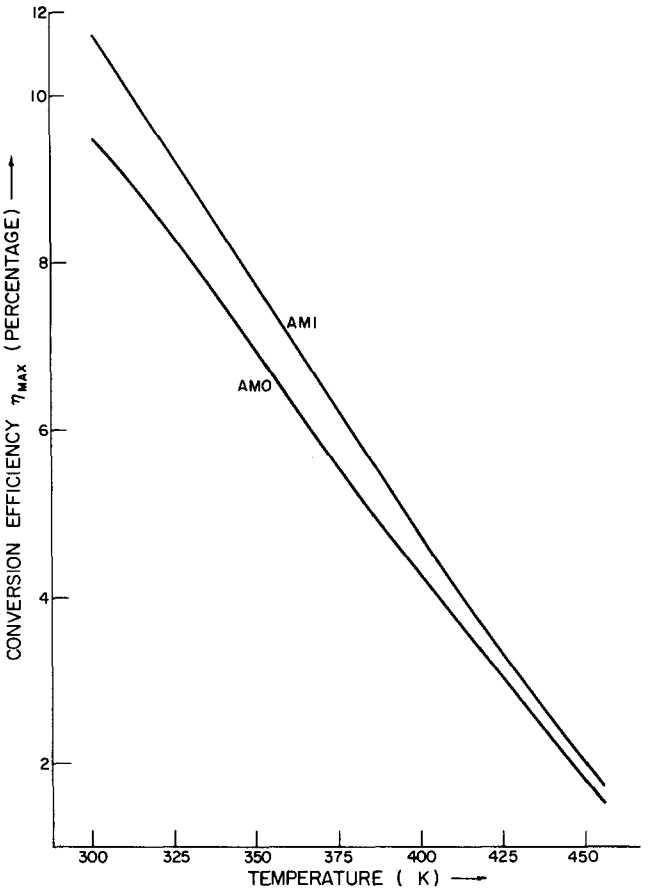

Fig. 2. Variation of maximum conversion efficiency of n^+p silicon solar cell with temperature at AM0 and AM1 solar spectrum.

References

[1] J. J. Wysocki and P. Rappaport, J. Appl. Phys. 31 (1960) 571.
[2] W. Luft, Advan. Energy Conversion 5 (1965) 21.
[3] R. K. Yasui and L. W. Schmidt, Conf. Rec. Eighth IEEE Photovoltaic Specialist Conf. (1970) p. 110.
[4] D. J. Curtin and R. W. Cool, Conf. Rec. Tenth IEEE Photovoltaic Specialist Conf. (1973) p. 139.
[5] L. J. Goldhammer and L. W. Slifer Jr., Conf. Rec. Twelfth IEEE Photovoltaic Specialist Conf. (1976) p. 199.
[6] A. Agarwal, V. K. Tewary, S. K. Agarwal and S. C. Jain, Solid-State Electron. 23 (1980) 1021.
[7] J. R. Hauser and P. M. Dunbar, IEEE Trans. Electron Devices ED-24 (1977) 305.
[8] D. W. Spaderna and D. H. Novan, IEEE Trans. Electron Devices ED-25 (1978) 1290.
[9] D. J. Roulston, N. D. Arora and S. G. Chamberlain, IEEE Trans. Electron Devices ED-29 (1982) in press.
[10] N. D. Arora, S. G. Chamberlain and D. J. Roulston, Appl. Phys. Lett. 37 (1980) 325.
[11] N. C. Wyeth, Solid-State Electron. 20 (1977) 629.
[12] J. R. Hauser and N. D. Arora, to be published.

[13] S. S. Li and W. R. Thurber, Solid-State Electron. 20 (1977) 609.
[14] S. S. Li, Solid-State Electron. 21 (1978) 1109.
[15] H. A. Weakliem and D. Redfield, J. Appl. Phys. 50 (1979) 1491.
[16] H. R. Phillip and E. A. Taft, Phys. Rev. 120 (1960) 37.
[17] C. E. Backus, Solar Cells (IEEE Press, New York, 1976) p. 1.
[18] N. D. Arora, S. G. Chamberlain and D. J. Roulston, University of Waterloo Tech. Report No. UWEE80-5 (April 1980).
[19] N. M. Ravindra and V. K. Srivastava, Solar Energy Mater. 2 (1979) 249.